Solar Energy Materials & Solar Cells 152 (2016) 73–79

Contents lists available at ScienceDirect

Solar Energy Materials & Solar Cells

journal homepage: www.elsevier.com/locate/solmat

Passivating contacts for silicon solar cells based on boron-diffused recrystallized amorphous silicon and thin dielectric interlayers

Di Yan, Andres Cuevas, Yimao Wan, James Bullock

Research School of Engineering, College of Computer Science and Engineering, The Australian National University, Canberra 0200, Australia

ARTICLE INFO

Article history:
Received 18 December 2015
Received in revised form
25 February 2016
Accepted 24 March 2016
Available online 7 April 2016

Keywords:
Boron
Amorphous silicon
Polysilicon
Passivated contact
Solar cell

ABSTRACT

A technique to make poly-Si (p^+)/SiO_x contacts for crystalline silicon solar cells based on doping PECVD intrinsic amorphous silicon (a-Si) by means of a thermal BBr_3 diffusion process is demonstrated. The thickness of the a-Si layer and the temperature of the boron diffusion are optimized in terms of suppressing carrier recombination and transport losses. Different interfacial layers are studied, including ultra-thin SiO_x grown either chemically or thermally, and stacks of SiO_x and SiN_x. While the double SiO_x/SiN_x interlayers do not achieve the desired performance, both kinds of single SiO_x layers produce satisfactory passivating contacts, with both a low recombination current and a low contact resistivity. By adjusting the boron diffusion temperature, recombination current parameter J_0 values of ~16 fA/cm^2 to ~30 fA/cm^2 have been obtained for structures with initial a-Si thicknesses of 36–46 nm, together with a contact resistivity of ~8 mΩ cm^2.

1. Introduction

Recombination at the interface between metal and silicon eventually limits the maximum attainable efficiency of conventional dopant-diffused silicon solar cells. Besides restricting the contact area and introducing a heavily doped region under the metal, placing a self-passivating layer between metal and silicon is an effective approach to overcome such limitations. Passivating contact structures based on an ultra-thin silicon oxide layer and a doped silicon layer having a polycrystalline, amorphous, or mixed phase are being actively developed. The implementation of such approach to the rear side of n-type silicon solar cells has recently led to a 25.1% conversion efficiency [1]. Based on different doping technologies, thermal diffusion [2,3], in-situ doping by CVD [4] and ion implantation [5–7], both n-type electron-selective and p-type hole-selective contacts have been formed. From these recent results, n-type silicon-film contact structures usually show a better passivating performance than p-type silicon-film passivating contacts. The n-type passivating contacts typically have a range of recombination current parameter values in the vicinity of ~10 fA/cm^2 [2–4,7] with one report of ~1 fA/cm^2 [5]. On the other hand, p-type passivating contacts typically present a higher recombination current of about ~20 fA/cm^2 [4,5,7] with one report of ~4.5 fA/cm^2 [5]. This difference in performance was already observed between p–n–p and n–p–n polysilicon emitter bipolar junction devices [8,9]. N-type polysilicon emitters have shown significant current gain enhancements, by a factor up to 30, while p-type polysilicon emitters can only increase the current gain by a factor of 10 [9]. Several explanations were offered in previous studies: boron has a larger diffusivity than phosphorus in polysilicon layers, fewer ionized boron atoms are segregated in the grain boundaries of polysilicon layers [9,10], the boron atom tends to induce more interface defects and oxide charges in the Si/SiO_2 interface system, due to the penetration of boron into the substrate [11].

In this work, we present a detailed study of p-type passivating contacts by means of boron diffusion, thin silicon dielectric layers, and amorphous silicon layers. The paths to obtaining an optimized p-type passivating contact are identified. There are three parameters that need to be investigated: the a-Si thickness, the interfacial layer, and the boron diffusion temperature. In those optimization steps, the recombination current parameter, sheet resistance and contact resistance are measured, as indicators of the self-passivating and selective transport qualities of an optimized structure. Firstly, the effect of a-Si thicknesses is investigated for three diffusion temperatures. Secondly, four different interfacial layers: a single chemical oxide, a single thin thermal silicon oxide, and two sets of SiN_x/chemical oxide double layers with SiN_x refractive index values of 2.5 and 3.0, are studied as a function of the boron diffusion temperature. The influence of a-Si thickness, interfacial layer conditions, diffusion temperature and low temperature anneal in forming gas (FGA) show a clear path to

E-mail address: u4299071@anu.edu.au (D. Yan).

http://dx.doi.org/10.1016/j.solmat.2016.03.033
0927-0248/

form optimized boron diffused poly-Si passivating contacts. In this work, we refer to the a-Si layer after the high temperature boron diffusion process as poly-Si, which is consistent with the terminology used in Ref. [12].

2. Experimental procedure

Samples for measuring the recombination parameter J_{0c}, and the contact resistivity ρ_c, were prepared separately. P-type FZ silicon wafers with high resistivity ($\sim$100 Ω cm) and thickness of 470 μm were used for measuring J_{0c}, while p-type FZ silicon wafers with low resistivity ($\sim$0.5–1 Ω cm) and thickness of 200–250 μm were prepared for ρ_c measurements. Two types of thin oxide layers were studied: a thin chemical oxide and a thermal oxide layer. A thickness of $\sim$1.4 nm chemical oxide was grown by immersing silicon wafers (both J_{0c} samples and ρ_c samples) into a 68 wt% nitric acid solution at a temperature of 90 °C. A thermal oxide layer with a similar thickness of $\sim$1–1.3 nm, was prepared thermally in a quartz tube by means of dry oxidation process at 600 °C. During the 400 °C PECVD film deposition, some of chemical oxide samples received a stack of SiN_x and a-Si:H layers, while other chemical oxide samples and all thermal oxide samples were coated with intrinsic a-Si only. Two different 14 nm thick SiN_x layers with refractive indices (at a wavelength of 632 nm) of 2.5 and 3.0 were deposited in the SiN_x/a-Si:H stack structure. The J_{0c} samples were prepared with a symmetrical layer structure on both sides, while the ρ_c samples had a one side passivating contact structure. After PECVD film deposition, both J_{0c} samples and ρ_c samples were doped with boron atoms by using BBr_3 as a diffusion source at a temperature ranging from 870 °C to 980 °C. A fixed 30 min of BBr_3 deposition and a subsequent 30 min drive-in in nitrogen at the same temperature were used for all diffusion temperatures.

After removing the boron silicate glass (BSG) layer, J_{0c} was measured at room temperature by transient photoconductance decay (PCD) [13] and quasi-steady state photoconductance (QSSPC) [14] at an excess carrier density in the range of $\Delta n = 0.5 - 1\times10^{15}cm^{-3}$, both before and after forming gas (95% Ar, 5% H_2) annealing (FGA) at 400 °C for 30 min. The Cox and Strack method was used to extract ρ_c values from the contact resistivity samples which have various sizes of circular aluminium contacts on top of the poly-Si layers [15]. Ten circular aluminium contacts with diameters of 0.06 ± 0.002 cm, 0.11 ± 0.002 cm, 0.15 ± 0.002 cm, 0.20 ± 0.004 cm, 0.24 ± 0.009 cm, 0.31 ± 0.02 cm, 0.41 ± 0.006 cm, 0.61 ± 0.004 cm, 0.79 ± 0.01 cm and 0.98 ± 0.08 cm, were fabricated. Error values, as indicated in the following figures, are calculated by accounting both errors of the wafer thickness and errors of the circular aluminium contact sizes. The resolution of the contact resistivity measurement strongly depends on the resistivity and thickness of the silicon substrate. In our case, the minimum contact resistivity that can be detected is 5 mΩ cm^2, indicated as dashed lines in the graphs that show the contact resistivity measurements. The electrically active boron dopant concentration in the p^+poly-Si/SiO_x contact structure was measured by the electrochemical capacitance–voltage technique (WEP Wafer Profile CVP21). The final dopant profiles were calibrated by the same scaling factor that is used to correct the boron dopant profiles in mono-crystalline silicon, which was determined by matching the boron dopant profile to the measured sheet resistance.

3. Optimization of the a-Si thickness and the boron diffusion

3.1. Dopant profile

After the growth of a $\sim$1.4 nm chemical oxide layer, the second step in the formation of the contact structure is to deposit a layer of un-doped a-Si. The thickness of this layer needs to be optimized in conjunction with the boron diffusion process. On the one hand, it is very important, as we shall see below, that the entirety of the silicon layer is doped with a high concentration of boron atoms. Some boron atoms diffuse across the thin oxide and into the silicon wafer, and this can also have an impact on the final performance of the contact. On the other hand, the boron diffusion consumes a certain amount of the deposited silicon, reducing the final thickness of the layer. In the BBr_3 diffusion process, boron oxide (B_2O_3) is formed on the silicon surface, and introducing boron into the silicon requires a surface reaction between B_2O_3 and silicon [16].

To explore such trade-off, we prepared samples with a-Si layer thicknesses of 29 nm, 36 nm, 46 nm, 55 nm and 90 nm, and subjected them to three different diffusion temperatures, 920 °C, 960 °C and 980 °C. The boron profiles corresponding to the lowest

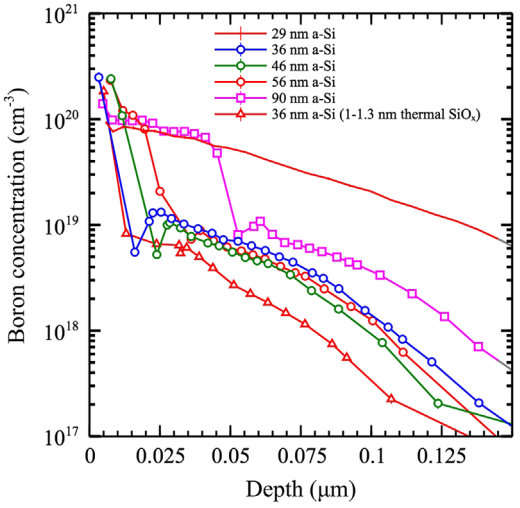

Fig. 1. Boron doping profiles of poly-Si/SiO_x/c-Si passivating contact at diffusion temperature of 920 °C for different thicknesses of the deposited a-Si layer.

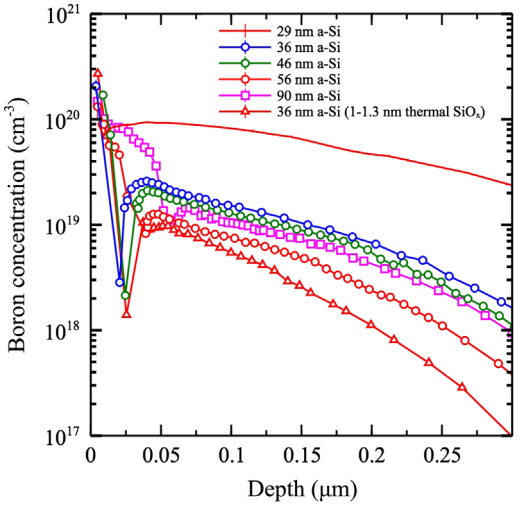

Fig. 2. Boron doping profiles of poly-Si/SiO_x/c-Si passivating contact at diffusion temperature of 980 °C for different thicknesses of the deposited a-Si layer.

Table 1
Summary of data for samples with four different initial a-Si thicknesses after boron diffusion at 920 °C and 980 °C, including the approximate poly-Si thickness extracted from the ECV measurements, the recombination current parameter in the boron doped region of the c-Si substrate J_{0bulk}, modeled from the ECV profiles, its percentage contribution to the total recombination current J_{0bulk}%, and the modeled effective surface recombination velocity, S_{eff}, before FGA at the c-Si/SiO_x interface.

a-Si thickness (nm)	Poly-Si thickness (nm)	BBr_3 temperature (°C)	J_{0bulk} (fA/cm^{-2})	J_{0bulk} (%)	S_{eff} (before FGA) (cm/s)
36	20	920	0.7	3.5	1143
46	24	920	0.4	1.7	1227
56	36	920	0.3	0.7	2535
90	53	920	0.4	0.2	6396
36	20.5	980	5.4	20.5	1410
46	24.5	980	3.8	14.2	1644
56	39	980	1.5	4.3	2007
90	52	980	1.9	3.0	3924

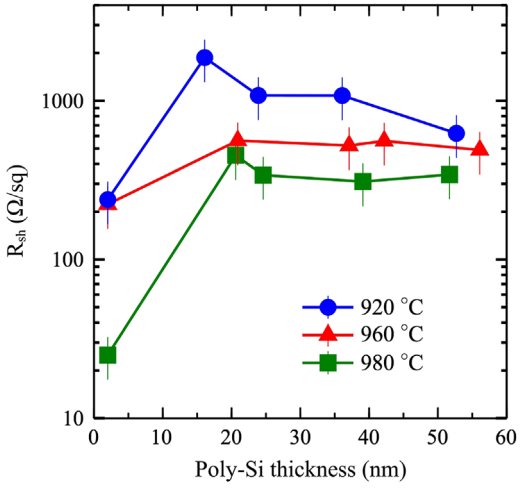

Fig. 3. Sheet resistance measurements of poly-Si/chemical SiO_x/c-Si as a function of the poly-Si thickness. They are shown for three different boron diffusion temperatures, 920 °C, 960 °C and 980 °C.

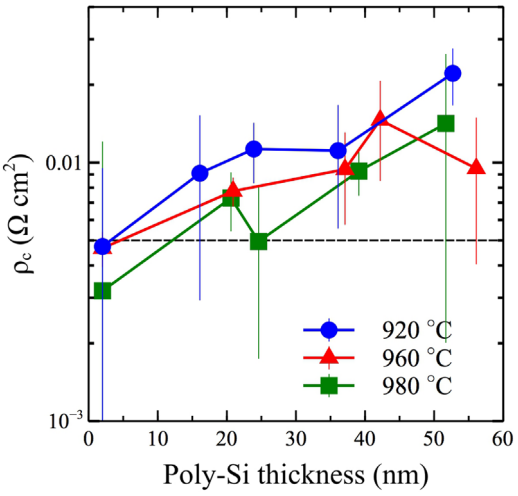

Fig. 4. Contact resistivity measurements of poly-Si/chemical SiO_x/c-Si as a function of the approximate poly-Si thickness for three different boron diffusion temperatures, 920 °C, 960 °C and 980 °C. The dashed line represents the lowest contact resistivity that can be reliably detected with the measurement technique used.

and highest temperatures, measured by ECV, are shown in Figs. 1 and 2, respectively. The first observation is that the measurement corresponding to the sample with the thinnest a-Si layer presents a Gaussian profile that is very close to the typical boron profile obtained on a mono-crystalline silicon wafer (i.e., without an a-Si layer) for those diffusion conditions. This indicates that the thin a-Si layer has probably been completely oxidized during the boron pre-deposition step. All the other samples present a qualitatively similar profile, having a high boron concentration near the surface followed by a sharp drop and then a moderate concentration "tail" into the silicon wafer, which is deeper for the higher diffusion temperature. Such sudden drop in boron concentration was also observed in the ECV profiles of boron implanted TOPCon structures [6]. The drop can be due to the diffusivity and the segregation coefficient of boron in the thin SiO_x and at the interfaces between poly-Si/SiO_x and SiO_x/c-Si, which differ from the values in mono-crystalline silicon. As indicated in Ref. [6], it is reasonable to identify the position of this sudden drop in boron concentration as the location of the interfacial SiO_x layer present between the poly-Si and the c-Si. As can be seen in Figs. 1 and 2, the interface position is deeper when the a-Si layer is thicker. The ECV measurement is therefore capable of revealing the presence, or not, and approximate thickness of the poly-Si layer. Approximate poly-Si thicknesses are listed in Table 1. Note that this method of estimating the poly-Si layer thickness is prone to error, compared to more precise microscopy methods, yet it is sufficient for the relative comparisons and experimental optimizations in this paper. Surprisingly, there is practically no additional a-Si consumed by increasing the boron diffusion temperature by 60 °C, since the thickness of poly-Si after 920 °C is very similar to the thickness of poly-Si after 980 °C. This contributes to making the contact resistivity weakly sensitive to the diffusion temperature. The absolute value of the boron concentration within the poly-Si is less reliable for the thinner than the thicker layers, but is in all cases $\sim 1–3 \times 10^{20}$ cm^{-3}. This is almost one order of magnitude higher than the boron concentration in the silicon substrate. The latter is lower, $\sim 0.7–1.5 \times 10^{19}$ cm^{-3}, for the samples doped at 920 °C than for those doped at 980 °C, where the boron concentration at the SiO_x/c-Si interface is $\sim 1–2.5 \times 10^{19}$ cm^{-3}. This drastic drop in boron concentration emphasizes the role of the thin interfacial oxide as a diffusion barrier, even though it does not completely block the diffusion of boron into the wafer.

3.2. Sheet resistance and contact resistivity

An additional evidence of the critical role of the interfacial layer is given by the measured sheet resistance, shown in Fig. 3. The sheet resistance R_{sh} corresponding to the samples with the thinnest poly-Si layer is very low, in correspondence with the deep and highly doped boron profiles shown in Figs. 1 and 2. For all the samples with an initial a-Si thickness greater than 36 nm (> 20 nm for the final poly-Si), the R_{sh} values are consistently large. This indicates that the thin chemical SiO_x layer is an effective barrier to the diffusion of boron atoms, even though there is a small number of them (the tail in the profiles) crossing into the silicon substrate. In agreement with the deeper profiles in Figs. 1 and 2, the R_{sh} value is reduced by approximately a factor of two as the diffusion temperature is increased.

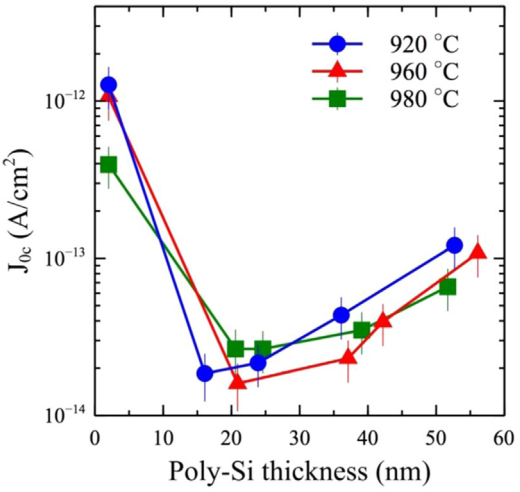

Fig. 5. Recombination current density of poly-Si/chemical SiO_x/c-Si passivating structures as a function of approximate poly-Si thickness for three different boron diffusion temperatures, 920 °C, 960 °C and 980 °C before FGA.

The measured contact resistivity, ρ_c, shown in Fig. 4 is also consistent with the depiction of the interface given above. When the final poly-Si layer is too thin, the contact resistivity is very low, down to the resolution limit of the technique used to measure it. This is consistent with the a-Si layer and the interfacial SiO_x having been consumed during the diffusion process. All other samples show contact resistivity values in the range of 5–14 mΩ cm^2, most likely limited by quantum mechanical tunneling through the thin SiO_x interlayer, as well as the bulk resistivity of boron doped poly-Si layers.

3.3. Recombination current density

Plots of the recombination current density parameter J_{0c} corresponding to the three diffusion temperatures of 920 °C, 960 °C and 980 °C as a function of the approximate poly-Si thickness are shown in Fig. 5. The samples on which the thinnest a-Si layers were deposited present very high J_{0c} values for all three diffusion processes, similar to those typically found for similar boron dopant profiles with no surface passivation. The recombination losses are drastically reduced by the presence of the poly-Si/SiO_x stack in all the other samples. The 920 °C and 960 °C boron diffusions result in the lowest recombination currents of ~18 fA/cm^2 and ~16 fA/cm^2 respectively, which are obtained for the samples with a relatively thin initial a-Si layer of 36 nm. J_{0c} increases with the thickness of the poly-Si layer, first marginally, up to an initial a-Si thickness of 46 nm, and then more markedly, for the samples on which the thickest a-Si layers were deposited. Increasing the diffusion temperature to 980 °C causes a small increase in recombination for the samples on which the thin a-Si layers were deposited, J_{0c} ~26.5 fA/cm^2 for 36 nm initial a-Si layer (~20.5 nm final poly-Si thickness), but it is beneficial for the thickest initial a-Si layers. The higher boron diffusion temperature of 980 °C is preferable for the 90 nm initial a-Si layer (~50 nm final poly-Si thickness) in order to introduce an appropriate amount of boron atoms throughout the thicker final poly-Si/SiO_x structure and thus reduce recombination, resulting in a J_{0c} of 70 fA/cm^2.

Given that the different diffusion temperatures result in significantly different boron concentration profiles, we investigated the possible contribution of the boron "tail" present in the silicon substrate in the total recombination. Similarly to the procedure in Ref. [7], we calculated the recombination current parameter J_{0bulk} due to bulk Auger recombination by assuming a zero surface recombination velocity at the internal interface SiO_x/c-Si. We used an analytic model for minority carrier transport [16] and the empirical parameterization of band gap narrowing in [17]. The results of the modeling are summarized in Table 1, both in absolute values and as a percentage of the total recombination current parameter J_{0c} of the contact structure. At the lower boron diffusion temperature, 920 °C, the dopant profiles in the silicon substrate are shallower and have a lower concentration, resulting in bulk recombination currents below 0.6 fA/cm^2, that contribute small percentages to the total J_{0c}, from ~1% to ~3.4%. In the case of 980 °C diffusion temperature, the higher dopant doses introduced into the wafer produce bulk recombination contributions of up to 5.4 fA/cm^2, which contribute ~14% and ~20% of the total J_{0c} measured for the 36 nm a-Si and 46 nm a-Si samples. The thicker a-Si layers present a greater impediment to boron diffusion and result in shallower dopant profiles in the silicon substrate, which contribute less than 4% to their total J_{0c}. This analysis indicates that Auger recombination can partially explain small differences observed for samples with the same a-Si layer doped at the two temperatures; for example, the 36 nm a-Si sample doped at 980 °C has ~5.4 fA/cm^2 higher Auger recombination that the sample doped at 920 °C, which nearly explains the difference between the respective J_{0c} ~26.5 fA/cm^2 and J_{0c} ~18.5 fA/cm^2.

The main conclusion of this analysis is that Auger recombination within the boron doped regions formed in the substrate cannot explain the measured J_{0c}. Therefore, it is necessary to invoke other recombination processes, such as possible carrier injection and recombination in the boron doped poly-Si layer, and interface recombination. In the modeling, all those processes can be lumped into an effective surface recombination velocity (S_{eff}) present at the SiO_x/c-Si interface. The S_{eff} values needed for the model to fully account for the measured J_{0c} are given in Table 1. It is beyond the scope of this paper to discriminate the physical mechanisms behind these S_{eff} values. In a possible scenario, we could conjecture that the probability for minority carrier tunneling through the interlayer is very low, in which case S_{eff} could be attributed exclusively to defect-mediated recombination at the SiO_x/c-Si interface. The modeling results shown in Table 1 indicate that relatively high values of S_{eff}, in the range ~1.1–6.4 × 10^3 cm/s before a forming gas anneal, are acceptable; that is, the requirements on interface passivation are relatively modest. Numerical simulation by other researchers [18] show that similar surface recombination velocities (from 10^3 cm/s to 10^4 cm/s) at the interface between the Si wafer absorber and the oxide layer are sufficient for guaranteeing high V_{oc} values (> 700 mV). This is possible thanks to the presence of the boron dopant tail in the near-surface region of the monocrystalline Si wafer. The analysis indicates that it is the combination of this dopant tail and a moderate level of interface passivation that results in a very low J_{0c}. Nevertheless, we cannot exclude that the actual interfacial recombination velocity may be lower than S_{eff} and that some minority carriers may leak into the polySi layer, either by tunneling or small pinholes in the SiO_x, and recombine there.

From these experiments, we can conclude that the performance of the p-type passivating contact is mainly determined by the amount of boron introduced in the poly-Si layer, at the SiO_x/c-Si interface and into the c-Si. Thus, both the a-Si thickness and the boron diffusion process are important parameters to be optimized. We found that the ideal a-Si thickness is in the range between 36 nm and 46 nm (approximate poly-Si thickness between ~20 nm and ~25 nm). At 960 °C, these poly-Si layers give a J_{0c} between 16 fA/cm^2 and 23 fA/cm^2, together with a contact resistivity of ~8 mΩ cm^2 to ~9.5 mΩ cm^2. At 980 °C, a slightly lower contact resistivity of 7.3 mΩ cm^2 and slightly higher J_{0c} of 26.5 fA/cm^2 were obtained for both the 36 nm and 46 nm initial a-Si layers.

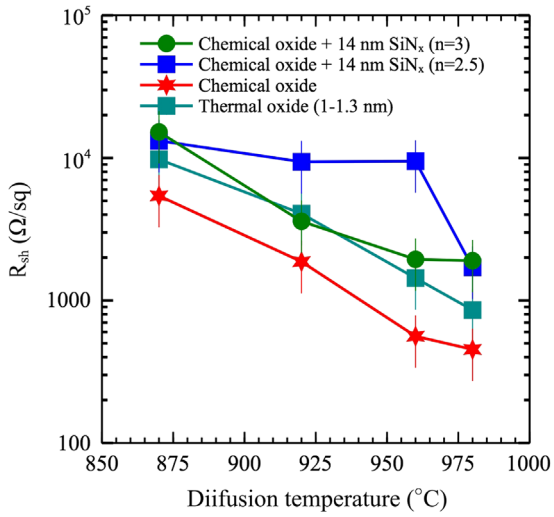

Fig. 6. Sheet resistance measurement of p^+ poly-Si/interfacial layers/c-Si structures as a function of BBr3 diffusion temperature. Four different interfacial layers: $n=2.5$ SiN_x/chemical SiO_x, $n=3.0$ SiN_x/chemical SiO_x, chemical SiO_x, and thermal SiO_x, were covered by 36 nm a-Si.

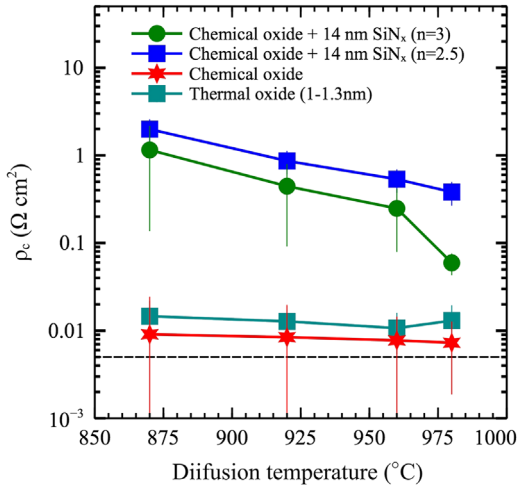

Fig. 7. Contact resistivity measurements of p^+ poly-Si/interfacial layers/c-Si structures as a function of BBr_3 diffusion temperature. There are four different interfacial layers, $n=2.5$ SiN_x/chemical SiO_x, $n=3$ SiN_x/chemical SiO_x, chemical SiO_x, and thermal SiO_x. All these samples received a-Si with a thickness of 36 nm. The dashed line represents the lowest contact resistivity that can be reliably detected with the measurement technique used.

4. Single and double interfacial layers

Given that in the previous section we only used a chemically grown SiO_x, it is worth exploring other interfacial layers to see if they may be advantageous. In this section we investigate thermally grown interfacial oxides with a thickness of ~1–1.3 nm. In addition, we also explore contact structures that include a double SiO_x/SiN_x interfacial layer. We have recently found that such double layers are beneficial in the case of phosphorus doped poly-Si contacts [12]. The double layers used here consist of a 1.4 nm chemical SiO_x plus a 14 nm SiN_x layer deposited by PECVD. For the latter we explore two different compositions, represented by refractive indices (measured at a wavelength of 632 nm) of $n=2.5$ and $n=3.0$. All these samples had the same a-Si layer deposited on top of the SiO_x or SiO_x/SiN_x stack by PECVD with a thickness of 36 nm (~20 nm poly-Si), which was found to be optimal in the previous section. The results of the experiments in terms of R_{sh}, ρ_c and J_{0c} as a function of boron diffusion temperature are shown in Figs. 6–8.

4.1. Sheet resistance and contact resistivity

In p-type polysilicon MOS technology, SiN_x/SiO_2 double layers have been used to suppress the penetration of boron atoms into the silicon substrate and thus improve the reliability of small scale MOS devices [19]. The diffusivity of boron through SiN_x films is hampered by the strength of the Si–N bonds, particularly abundant in material compositions characterized by a low refractive index. It has been documented that more energy is required to substitute a boron atom into a Si–N site than into a nitrogen free site [20,21]. Thus, a higher blocking ability of boron diffusion can be expected for films with a high nitrogen concentration (low refractive index) that those with a relatively high silicon concentration (high refractive index). Our experiments confirm that the double layer based on SiN_x with a refractive index of 2.5 is indeed a very effective barrier to the diffusion of boron up to a temperature of 960 °C, as demonstrated by the very high R_{sh} measured for such samples. The more silicon rich, $n=3.0$, SiN_x/chemical SiO_x double layer has a reduced blocking ability, no much better than that offered by a single ~1–1.3 nm SiO_x layer (see Fig. 6), except at the highest diffusion temperature. At 980 °C the $n=3.0$ and $n=2.5$ SiN_x layers result in approximately the same R_{sh}, indicating significant boron penetration, but still to a lesser degree than for the single oxide layers. The latter are quite different, the chemical SiO_x being less efficient at impeding boron diffusion than the thermal SiO_x, which results in R_{sh} values approximately a factor of 2 higher.

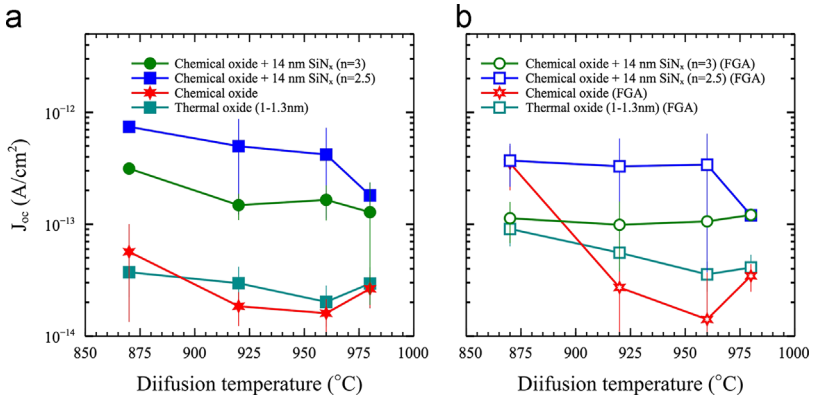

Fig. 8. Recombination current density of p^+ poly-Si/interfacial layers/c-Si structures as a function of the BBr_3 diffusion temperature. Four different interfacial layers: $n=2.5$ SiN_x/chemical SiO_x, $n=3$ SiN_x/chemical SiO_x, chemical SiO_x, and thermal SiO_x, were coated with 36 nm a-Si. (a) Indicates the recombination current densities before FGA and (b) after FGA. (For interpretation of the references to color in this figure, the reader is referred to the web version of this article.)

The contact resistivity measurements, shown in Fig. 7, indicate that the double SiN_x/SiO_x interfacial layers present a high resistance to the flow of current through them, particularly when the refractive index of the SiN_x is low. The higher refractive index SiN_x ($n=3.0$) gives a lower ρ_c, which follows a decreasing trend with diffusion temperature. This behavior is consistent with an increasing boron penetration into and through the silicon rich SiN_x, which results in an enhanced conductivity of the poly-Si/SiN_x/SiO_x structure. Nevertheless, only the samples diffused at 960–980 °C achieve a sufficiently low ρ_c for a full area solar cell contact. On the other hand, the samples with a single silicon oxide layer, either chemical or thermal, achieve a low contact resistance in the range of from $\sim$7 mΩ cm^2 to 20 mΩ cm^2. The diffusion temperature does not have a large impact on ρ_c. Such insensitivity of ρ_c to the diffusion temperature can be partly explained by the limitations of the technique used to measure it, indicated by the dashed line in Figs. 4 and 7. Once the contact resistivity approaches such limit, there are large errors in its extraction, as indicated by the large error bars in Fig. 7. The thermal SiO_x results in slightly higher ρ_c values than the chemical SiO_x, possibly related to its higher density, which in turn leads to a smaller concentration of boron at the interface between the thermal oxide layer and the silicon substrate. As illustrated by the doping profiles in Figs. 1 and 2, there are small variations in the boron concentration in the polysilicon and at the interface between SiO_x and c-Si when increasing the diffusion temperature from 920 °C to 980 °C. For a-Si with initial thickness 36 nm and chemical oxide, $N_{interface}=1.08\times10^{19}$ cm^{-3} at 920 °C and $N_{interface}=1.45\times10^{19}$ cm^{-3} at 980 °C; for a-Si with initial thickness 36 nm and thermal oxide, $N_{interface}=8.27\times10^{18}$ cm^{-3} at 920 °C and $N_{interface}=1.05\times10^{19}$ cm^{-3} at 980 °C. This indicates that a higher boron concentration at the interface helps to reduce the global contact resistivity of the structure.

4.2. Recombination current

The J_{0c} values of the above four groups of samples before and after FGA are shown separately in Fig. 8a and b. The samples with double SiN_x/chemical SiO_x layer (blue square for $n=2.5$ and green circle for $n=3$) have larger recombination than the samples with single SiO_x interfacial layers (red asterisks for the chemical SiO_x and teal square for the thermal SiO_x). The same observation was made for the n-type phosphorus diffused contact structures presented in [12]. The more effective boron blocking layers (SiN_x with $n=2.5$) result in very high J_{0c} values, except for the 980 °C diffusion case, when such blocking ceases and the sheet resistance drops (see Fig. 6). The more silicon rich SiN_x with $n=3.0$ gives significantly lower J_{0c}, parallel to the lower R_{sheet} and higher doping it permits. Nevertheless, such J_{0c} is still above $\sim$100 fA/cm^2, much higher than the values achieved by the single SiO_x interfacial layer samples. As mentioned in the previous section, the lowest J_{0c} value of $\sim$16 fA/cm^2 is obtained for the single chemical SiO_x at a diffusion temperature of 960 °C. The thermal SiO_x samples have slightly higher J_{0c} values, quite consistent between 20 fA/cm^2 and 37 fA/cm^2 for diffusion temperatures from 870 °C to 980 °C. A similar behavior was observed in the phosphorus diffused n-type passivating contacts based on a-Si and 1.3 nm thermal SiO_x layer [12].

After FGA at 400 °C, as indicated in Fig. 8b, there is a pronounced degradation in the samples with single interfacial layers (open red asterisks for the chemical SiO_x and open teal square for the thermal SiO_x). After FGA, J_{0c} values consistently increase by a factor of two on the single thermal SiO_x samples. In the samples with single chemical SiO_x interfacial layers, the level of degradation of J_{0c} varies with the diffusion temperature, being a large 351 fA/cm^2 at the lowest diffusion temperature (870 °C) and negligible at the highest diffusion temperatures (960 °C and 980 °C). The fact that a FGA causes an increase in recombination is contrary to expectations, even though it was also observed for similar structures doped with phosphorus [12]. On the other hand, the samples with a double SiN_x/SiO_x interlayer do respond to hydrogenation in the way that is normally expected, that is, with a reduction in interface recombination. A factor of 2 improvement has been observed on the samples with $n=3.0$ SiN_x/SiO_x (open green circles) and $n=2.5$ SiN_x/SiO_x double layer (open blue squares). However, this improvement is not as significant as what was observed for phosphorus doped structures, and the J_{0c} values of the p^+polySi/SiN_x/SiO_x structures remains higher than for those with a single SiO_x layer.

From the above comparison between the four interfacial conditions, we can conclude that the chemical SiO_x layer is globally the best in terms of recombination, contact resistivity and stability after FGA. The p^+poly-Si/SiO_x structure with a thermal SiO_x layer has a similar performance to the chemical SiO_x before FGA, but it degrades after FGA. The SiN_x/chemical SiO_x double layer samples show high recombination currents (>100 fA/cm^2) and contact resistances (>100 mΩ cm^2), even though they improve after FGA. Therefore, the optimized p-type passivating contact should have a chemical oxide as an interfacial layer and an initial a-Si layer approximately 36 nm thick. A J_{0c} value of $\sim$16 fA/cm^2 with contact resistivity of 8 mΩ cm^2 can then be obtained at a boron diffusion temperature of 960 °C.

5. Conclusion

An approach to form p-type passivating contacts based on PECVD of undoped amorphous silicon followed by thermal diffusion of boron from a BBr_3 source has been demonstrated. The detailed optimization of the process has included modifying the a-Si thickness, the diffusion temperature and the interfacial layer. Firstly, the behavior of these boron doped passivating contacts as a function of a-Si thickness has indicated that, to ensure both a low recombination current and a low contact resistivity, it is important to keep a moderate doping level in the poly-Si/SiO_x structure, aiming for a high doping concentration in the poly-Si region and at both sides of the interfacial layer, together with a low doping tail within the silicon substrate. Thin a-Si layers with initial thickness of 29 nm are completely oxidized, leading to over doping, while the thicker a-Si layers require a higher boron diffusion temperature to reach an optimized doping level. Modeling indicates that the tail of boron doping into the c-Si wafer is not the cause for the relatively high recombination currents observed in some samples, particularly in those with the thicker a-Si layers. Hence recombination in such samples is most likely dominated by processes occurring at the interfaces or in the boron doped poly-Si.

By comparing four different interfacial layers as a function of diffusion temperature, we confirmed that a double SiN_x/chemical SiO_x layer suppresses the penetration of boron into the silicon substrate. The performance of such layers improves after FGA, but not sufficiently to make them attractive. In particular, their contact resistance is very high, probably due to an insufficient doping of both sides of the interfacial layers. A better performance can be achieved with a single SiO_x interfacial layer, which achieves much lower J_{0c} and ρ_c values, thanks to some boron diffusing across it and into the c-Si wafer. This means that it is necessary to have boron atoms filling the complete poly-Si/interfacial layer/c-Si stack structure for an optimized p-type passivating contact. Some degradation of J_{0c} after FGA was observed in the samples with either a single thermal silicon oxide or a single chemical silicon oxide. Nevertheless, the effect of the FGA can be eliminated by increasing the boron doping level in the structure. By adjusting the

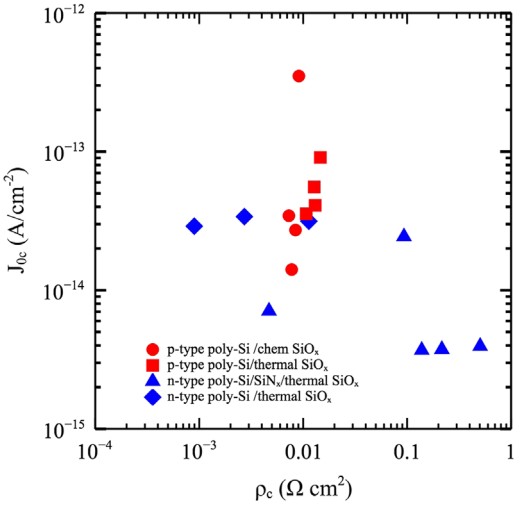

Fig. 9. Summary of contact resistivity and recombination current parameter pairs for n-type passivating contacts in Ref. [12] and p-type passivating contacts in this work. The J_{0c} values are given after FGA.

boron diffusion temperature to 960 °C or 980 °C, low recombination current parameters from ~16 fA/cm^2 to ~27 fA/cm^2 have been obtained for samples with initial a-Si thicknesses of 36 – 46 nm (approximate poly-Si thicknesses of ~20 nm and ~25 nm respectively). These low recombination losses are accompanied by a low contact resistance of ρ_c~8 mΩ cm^2. Such combination places this structure among the best options available to form self-passivating contacts for the selective transport of holes in silicon solar cells.

Finally, a summary of contact resistivity and recombination current density values of both n-type passivating contacts presented in Ref. [12] and p-type passivating contacts developed in this work is shown in Fig. 9. Both of them have been fabricated by means of a thermal diffusion process and PECVD deposited a-Si films. The differences between p-type poly-Si contacts and n-type poly-Si ones are pronounced, in terms of recombination current and contact resistivity parameters. Phosphorus doped poly-Si contacts achieve much lower J_{0c} values, but with a large scattering of the corresponding contact resistivity values. This is mainly due to the double SiN_x/SiO_x interfacial layer used for these n-type poly-Si contacts. Boron doped poly-Si contacts have a consistently low level of contact resistivity, with slightly higher J_{0c} values. These results match the conclusions of previous works, which have also found that n-type silicon-film contact structures usually show a better passivating performance than p-type silicon-film contacts. Nevertheless, the boron doped poly-Si contacts presented here open the way for fabricating effective hole-selective passivating contacts for high efficiency silicon solar cells.

Acknowledgments

This work has been supported by the Australian Renewable Energy Agency (ARENA) via the Australian Centre for Advanced Photovoltaics (ACAP). Facilities at the Australian National Fabrication Facility were used for some of the experimental work.

References

[1] S. Glunz, F. Feldmann, A. Richter, M. Bivour, C. Reichel, H. Steinkemper, et al., The irresistible charm of a simple current flow pattern – 25% with a solar cell featuring a full-area back contact, in: Proceedings of the 31st European Photovoltaic Solar Energy Conference and Exhibition, Hambury, Germany, 2015.
[2] U. Römer, R. Peibst, T. Ohrdes, B. Lim, J. Krügener, E. Bugiel, et al., Recombination behavior and contact resistance of n$^+$ and p$^+$ poly-crystalline Si/mono-crystalline Si junctions, Sol. Energy Mater. Sol. Cells 131 (2014) 85–91.
[3] D. Yan, A. Cuevas, J. Bullock, Y. Wan, C. Samundsett, Phosphorus-diffused polysilicon contacts for solar cells, Sol. Energy Mater. Sol. Cells (2015).
[4] F. Feldmann, M. Bivour, C. Reichel, M. Hermle, S.W. Glunz, Passivated rear contacts for high-efficiency n-type Si solar cells providing high interface passivation quality and excellent transport characteristics, Sol. Energy Mater. Sol. Cells 120 (Part A) (2014) 270–274.
[5] U. Romer, R. Peibst, T. Ohrdes, B. Lim, J. Krugener, T. Wietler, et al., Ion implantation for poly-Si passivated back-junction back-contacted solar cells, IEEE J. Photovolt. 5 (2) (2015) 1–8.
[6] F. Feldmann, R. Müller, C. Reichel, M. Hermle, Ion implantation into amorphous Si layers to form carrier-selective contacts for Si solar cells, Phys. Status Solidi (RRL) – Rapid Res. Lett. 08 (2014) 767–770.
[7] D.L. Young, W. Nemeth, V. LaSalvia, R. Reedy, S. Essig, N. Bateman, et al., Interdigitated back passivated contact (IBPC) solar cells formed by ion implantation, IEEE J. Photovolt. 6 (1) (2015) 1–7.
[8] I.R.C. Post, P. Ashburn, Investigation of boron diffusion in polysilicon and its application to the design of p–n–p polysilicon emitter bipolar transistors with shallow emitter junctions, IEEE Trans. Electron Devices 38 (1991) 2442–2451.
[9] C.M. Maritan, N.G. Tarr, Polysilicon emitter p–n–p transistors, IEEE Trans. Electron Devices 36 (1989) 1139–1144.
[10] K. Park, S. Batra, S. Banerjee, G. Lux, R. Manukonda, Comparison of arsenic and boron diffusion in polycrystalline/single-crystal silicon systems, J. Electrochem. Soc. 138 (1991) 545–549.
[11] J. Snel, The doped Si/SiO$_2$ interface, Solid-State Electron. 24 (2) (1981) 135–139.
[12] D. Yan, A. Cuevas, Y. Wan, J. Bullock, Silicon nitride/silicon oxide interlayers for solar cell passivating contacts based on PECVD amorphous silicon, Phys. Status Solidi (RRL) – Rapid Res. Lett. 9 (2015) 617–621.
[13] D.E. Kane, R.M. Swanson, Measurement of the emitter saturation current by a contactless photoconductivity decay method, in: Proceedings of IEEE Photovoltaic Specialists Conference, 1985.
[14] R.A. Sinton, A. Cuevas, M. Stuckings, Quasi-steady-state photoconductance, a new method for solar cell material and device characterization, in: Proceedings of the Twenty Fifth IEEE Conference Record of the Photovoltaic Specialists Conference, 1996, pp. 457–460.
[15] R.H. Cox, H. Strack, Ohmic contacts for GaAs devices, Solid-State Electron. 10 (12) (1967) 1213–1218.
[16] R.C. Jaeger, Introduction to Microelectronic Fabrication, Addison-Wesley Publishing Company, 1988.
[17] D. Yan, A. Cuevas, Empirical determination of the energy band gap narrowing in p$^+$ silicon heavily doped with boron, J. Appl. Phys. 116 (2014) 194505.
[18] H. Steinkemper, F. Feldmann, M. Bivour, M. Hermle, Numerical simulation of carrier-selective electron contacts featuring tunnel oxides, IEEE J. Photovolt. 5 (2015) 1348–1356.
[19] Y. Wu, G. Lucovsky, H.Z. Massoud, Improvement of gate dielectric reliability for p/sup +/ poly MOS devices using remote PECVD top nitride deposition on thin gate oxides, in: Proceedings of the 36th Annual IEEE International Reliability Physics Symposium, 1998, pp. 70–75.
[20] K. Ellis, R. Buhrman, Boron diffusion in silicon oxides and oxynitrides, J. Electrochem. Soc. 145 (1998) 2068–2074.
[21] W. Beall Fowler, A.H. Edwards, Theory of defects and defect processes in silicon dioxide, J. Non-Cryst. Solids 222 (1997) 33–41.